

# Dynamic Wavelet Coherence Maps and Frequency-Dependent Connectivity Strength in Default Mode Network

Hsu-Lei Lee<sup>1</sup>, Jakob Assländer<sup>1</sup>, Pierre LeVan<sup>1</sup>, and Jürgen Hennig<sup>1</sup>

<sup>1</sup>Medical Physics, University Medical Center Freiburg, Freiburg, BW, Germany

**Introduction** Resting-state fMRI is performed in the absence of specific cognitive tasks, where the baseline human brain activity is reflected in the spontaneous BOLD signal fluctuations<sup>1</sup>. Common resting-state studies analyze signals below 0.1 Hz acquired by conventional echo-planar imaging and assumed stationary networks during the entire scan. Recently time-frequency analysis of rs-fMRI data has received growing interests, with methods like wavelet coherence<sup>2</sup>, co-activation pattern analysis<sup>3</sup>, etc. emerging. Using wavelet transform coherence (WTC) we can obtain multi-resolution results with progressive window lengths and have greater flexibility to assess temporal-spectral relations between brain regions. In this study we used ICA and WTC on MR-Encephalography<sup>4</sup> (MREG) resting-state data to look at the connectivity change of brain regions in both temporal and spectral dimensions.

**Methods** Resting-state fMRI data from ten healthy volunteers were collected on a 3.0 T Siemens Trio scanner (Siemens Healthcare, Erlangen, Germany) with a 32-channel head coil. Subjects were instructed to close their eyes and relax during the scan session. MREG sequence with single-shot stack of spirals trajectory and a TR of 100 msec was used. In each session 4096 time frames were acquired (total scan time 6 min 50 sec), and the first 15 sec were discarded for signal stability consideration. Imaging volume FOV =  $192 \times 192 \times 192$  mm<sup>3</sup> and was reconstructed into a  $64 \times 64 \times 64$  matrix using forward operator estimated from a non-uniform FFT (nuFFT) algorithm based on coil sensitivity weightings and measured gradient trajectory<sup>5</sup>.

All post-processing was done in MATLAB (The Mathworks, Inc., Natick, MA). Reconstructed time-series were corrected for rigid-body motion with SPM8 (<http://www.fil.ion.ucl.ac.uk/spm>) and fed into GIFT toolbox (<http://icatb.sourceforge.net/>) to be separated into 60 components based on Infomax algorithm. 36 out of these 60 components were manually selected as neural-activity relevant nodes and used for further analysis. The wavelet coherence coefficients between each pair of nodes' time courses were then calculated using a Morlet wavelet with  $\omega_0 = 6$ <sup>6,7</sup>. We defined the network connectivity strength as the mean value of coherence coefficients between all nodes that belong to the same resting-state network:  $\frac{1}{n} \sum_{i,j} R^2_{i,j}(t,s)$ ,  $i,j \in \text{network}$  where  $R^2$  is the wavelet coherence coefficients that are above a 0.05 significance level<sup>5</sup> at each particular time( $t$ ) and frequency( $s$ ) point and  $n$  is the number of components in the current network.

**Results** Sample time frames of the coherence maps at different frequencies corresponding to default mode network (DMN) nodes (posterior cingulate, PCC and medial prefrontal cortex, mPFC) from one representative subject are shown in Figure 1a. The coherence coefficient and cross-wavelet phase are represented by value and hue in HSV color space, respectively. The time courses of the coherence between reference and other selected nodes are plotted in Figure 1b-1e. Figure 2a shows an example of the temporal-spectral variation of mean coherence strength within the default mode network. The group mean and standard deviation of the coherence coefficients with respect to frequency were calculated across all time points/subjects and are shown in Figure 2b.

**Discussion** The coherence maps with respect to PCC and mPFC show varying coherence strength and cross-wavelet phase in different DMN sub-regions. At 0.05 Hz strong coherence between DMN components can be seen with phase shifts falling mostly into  $-\pi/2 \sim \pi/2$  range. Regions like postcentral cortex and insula also have significant coherence at certain time points but with phase shifts around  $\pi$ , which can roughly be related to a negative local correlation coefficient. At 1.5 Hz the two reference nodes have fewer coherent components both within and outside DMN. The duration when there is significant coherence is reduced especially in the negatively correlated parts. However the cross-wavelet phases are more stable during those periods of coherence (Fig.1b&1d, red & orange dots). An abrupt drop of DMN connectivity strength after about 0.5 Hz can be observed in the group mean spectrum in Figure 2.

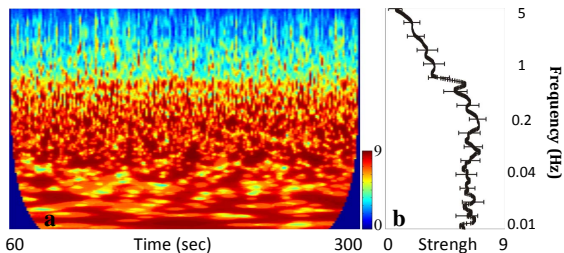


**Figure 2** Left: connectivity strength of DMN as a function of time and frequency from one representative subject. Right: Group mean and standard deviation of the within-network connectivity strength as a function of frequency.

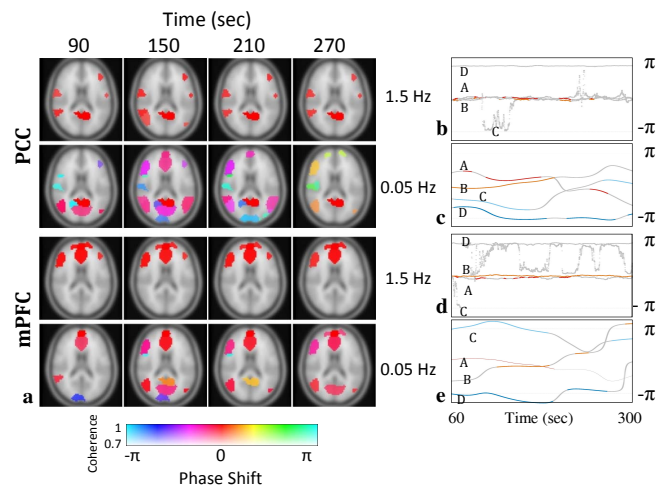


**Figure 1** (a) Coherence maps at different time points/ frequencies corresponding to PCC (top 2 rows) / mPFC (bottom 2 rows). (b)-(e): A(red)-cross-wavelet phase between PCC & mPFC as a function of time, B(orange)-angular gyrus, C(cyan)-postcentral cortex, D(blue)-insula. Data points in grey indicate there is no significant coherence at this location.

**Conclusion** Wavelet analysis provides adaptive temporal-spectral resolution which allows easy visualization and assessment of dynamic coherence information in individual subject as well as group data. Using wavelet coherence we demonstrated the frequency-dependent connectivity behaviour of DMN, where the connectivity strength decreases as signal frequency increases. In the future we will also study other resting-state networks and look to determine possible spectral characteristics of different networks.

**References** [1] Biswal *et al.*, MRM 34: 537-541 (1995); [2] Chang and Glover, NeuroImage 50:81-98 (2010); [3] Liu and Duyn, Proc. Natl. Acad. Sci. USA, 110:4392-4397 (2013); [4] Hennig *et al.*, NeuroImage, 34:212-219 (2007); [5] Grotz *et al.*, MRM 62:394-405 (2009); [6] Grinsted *et al.*, Nonlinear Process. Geophys., 11:561-566 (2004); [7] Muller *et al.*, J. Magn. Reson. Imaging 20:145-152 (2004). **Acknowledgement** This work was supported by the European Research Council Advanced Grant agreement 232908 "OVOC" and DFG Cluster of Excellence EXC-1086 "Brain Links-Brain Tools".